Non-Invasive Wireless IoT Oil Level Monitor Node using Submersible Sensors for Early Leak Detection

John Paul P. Caña
School of Graduate Studies
School of Electrical, Electronics and Computer Engineering
Mapua University
Manila, Philippines
jppcana@mymail.mapua.edu.ph

Jocelyn F. Villaverde
School of Electrical, Electronics and Computer Engineering
Mapua University
Manila, Philippines
jfvillaverde@mapua.edu.ph

***Abstract*—The early detection of safety critical conditions of oil levels in legacy industrial or commercial hydraulic machinery is becoming a new requirement for cloud-based maintenance service and Smart Grid systems. Building communities integrate accurate smart sensors to enable near or real-time monitoring. The non-ideal conditions of oil levels can lead to disastrous costly events. However, legacy systems have gone expensive rigorous safety qualifications, to alter them makes the integration of new IoT monitors a difficult decision. To avoid or mitigate safety related recertification, two test setups are proposed to determine the sensor accuracy: (1) Full-range liquid height level test at room temperature and (2) Limited-range height level test at varying temperatures to characterize its non-linearity effects on the sensor accuracy. During the empirical testing to obtain an optimal solution, the study proposes the use of Design for Six Sigma (DFSS) statistical method, an industry best-practice methodology to minimize parametric variations -by design- and increase the accuracy through measurements of variability and central tendency. Initially, the measured data drifted more than 50 percent from the desired values for both temperature and height readings. After the optimization, the temperature performance improved to a tighter specification of 0.25 percent from the initial prerequisite of 5 percent while the height performance improved from 8 percent starting requirement to 5 percent optimal specification. The DFSS empirical test is an effective method to achieve repeatable highly accurate oil level monitor.**

Keywords—Internet of Things, Wireless Network, Nodes, Liquid Level Measurement, Sensors

I. INTRODUCTION

Today, wireless Internet of Things (IoT) smart sensors are increasingly needed to monitor and send vital information in real or near real-time about the conditions of safety critical assets or equipment [1-2]. Various data types are collected by smart sensors to solve numerous issues such as traffic conditions, farming conditions, and industrial equipment status such as tunnel frame integrity, safety-critical hydraulic levels of pumps and elevators, etc [4-7]. The non-ideal conditions of oil levels used in commercial and industrial hydraulic applications such as hydraulic elevators and oil pump reservoirs could lead to safety concerns, loss of lives, and loss of profitability. Monitoring these reservoirs for low oil level due to leaks is becoming more critical. Service companies are improving their predictive maintenance systems continually with more dynamic oil level monitoring and early leak detection mechanisms to prevent a catastrophic event and provide a more value-add maintenance service to their customers. New approaches in building communities include smart sensors providing real-time monitoring and control [8-12]. Introducing some of these approaches, however, prove difficult specially to existing legacy systems as they may require physical alterations of pipes and tanks during the sensor integration process, resulting to consequential expensive safety related regulatory recertification. This study proposes a wireless IoT node sensor that requires less or no change to the structural integrity of the liquid reservoir. Instead of using inline sensors that may be installed in the pipe or in the tank, the concept instead includes a sensor device with an extended cable that can be easily placed onto the top lid of the tank that may not be safety regulated. Consequently, this does not require changing the structural integrity of the tank or the pipes. It also proposes the use of an industry best practice method in minimizing the reading variations at their roots to make the sensor highly accurate.

II. METHODOLOGY

This study follows the Design for Six Sigma (DFSS) methodology which is a proactive empirical approach to minimize the effects of non-linearities in components with high degree of performance. It uses quantifiable parameters taken from multiple measured data and conducting additional statistical work from the outset to control the factors that will produce consistent accurate results. It is an approach to product design that comes with several roadmaps. Though not all of the DFSS processes in commercial applications are used, this study follows the Define, Measure, Analyze, Design, and Verify (DMADV) methodology to ensure that the key parameters are considered and their potential causes for defects and variations are minimized at their roots. The DMADV process is as follows: (1) Define the constraints of the problem and the requirement of the sensor nodes in a simulated environment, (2) Measure the variability and central tendency performance of the components, (3) Analyze and evaluate the data collected during the characterization of the components and compare them with the expected critical requirements, (4) Design and assemble a sensor node prototype with the use of a development kit, submersible sensors, and 3D printed enclosures to demonstrate the reading accuracy and ease of installation concept, and (5) Verify the design through empirical testing adjusting the parameters that control the performance of the sensors, as required. The output of the process is an easy-to-install optimal solution for use in smart remote liquid level monitor and early leak detection of oil in hydraulic systems.

The conceptual framework of this study is the Input – Process – Output (IPO) Model to group the tasks or processes accordingly. The Input consists of a (1) Temperature Sensor Voltage Reading and a (2) Hydrostatic Sensor Voltage Reading. The Output involves the display of oil temperature and level reading in real time through a HyperTerminal tool taken from the submersible liquid level and temperature sensors (Input sources). The Process involves the DMADV methodology as described above.

The Prototype Concept, Requirements and Test Setups

The prototype design concept in Fig. 1 illustrates the budgetary industrial design (ID) of the Oil Level Monitor (OLM). The prototype is made of the System-On-Chip (SOC) development kit with Negative Thermal Coefficient (NTC) thermistor and hydrostatic liquid level sensors. It needs to be non-invasive, i.e., the node is easily installed with no change to the structural integrity of the tank. Instead of using inline sensors that may be installed in the pipe or in the tank, the concept instead includes a sensor device with an extended cable that can be easily placed onto the top lid of the tank that may not be safety regulated. Consequently, this does not require changing the structural integrity of the tank or the pipes.

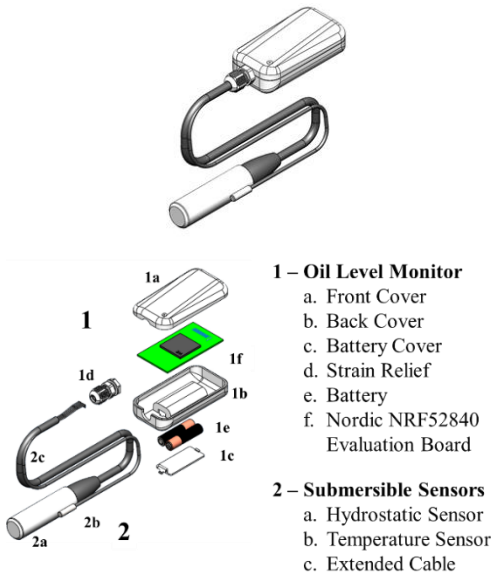

Figure 1. Prototype Concept ID of the OLM

Using a Nordic nRF52840 SOC as the processing unit, the main board of the sensor device is housed in a custom 3D printed enclosure. The sensor transducers at the end of the cable are submerged at the bottom of the tank while the monitor unit that houses the electronics is placed onto the lid or any structure outside close by the tank, as shown in Fig. 2, setup 1.

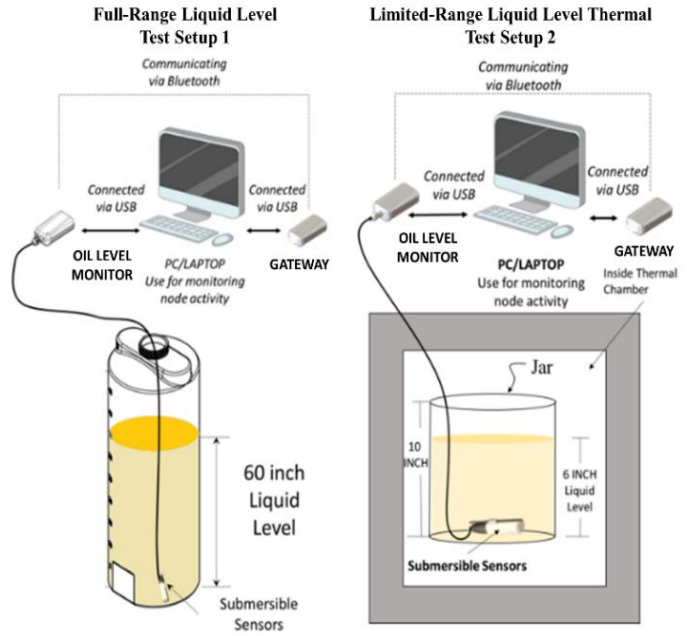

Figure 2. Hydrostatic Liquid Level Test Setups 1 & 2

The height level and temperature sensor readings need to measure a 60-inch-high tank across -15 °C to 70 °C within ±8% and ±5%, respectively. The sensors need to perform accurately and reliably within the specified thermal conditions. To test the performance capability within the limits of a simulated environment, two test setups are necessary due to the thermal chamber size constraints. As shown in Fig. 2, the first is the Full-Scale Liquid Level Setup 1 which measures at room temperature the reading of the submersible sensor across the range specified for the Hydrostatic sensor (0~60 inches). The second is the Thermal Characterization Setup 2, which measures the reading accuracy of the submersible sensor at a limited liquid level range from 2 to 6 inches. This is to assess the accuracy of the measured reading when subjected to temperatures from -15 °C to 70 °C.

The equipment used is listed in Table 1 below:

TABLE I. OIL LEVEL MONITORING TEST EQUIPMENT

Equipment	Model No.	Test Description
Digital Multi-meter (DMM)	Fluke 289	Measures the temperature and voltage level
Power Supply	BK Precision 9111	Provides power source to the devices; used as a test input source to the ADC
Thermal Chamber	Tenney Junior Temperature Test Chamber	Simulates varying thermal conditions.
PC/Laptop	Lenovo	Monitors the liquid level and temperature reading of the device.
Hydraulic Oil	AW-32, O'Reilly	ISO 32 Hydraulic oil
2-m tall liquid level container, 50 Gallon	Norwesco White Vertical Storage Tank 41865	Simulates hydraulic oil tank 18" Diameter x 80" Height

System Block Diagram

The system block diagram in Fig. 3a shows the major components in the design. Two separate sensors are used to measure the temperature and the liquid level. The analog signal received from the sensors are then processed by the ADC to translate the measured data into a machine language. After the processor calculates the right data translation, the data is sent via Bluetooth and displays the information using the laptop HyperTerminal.

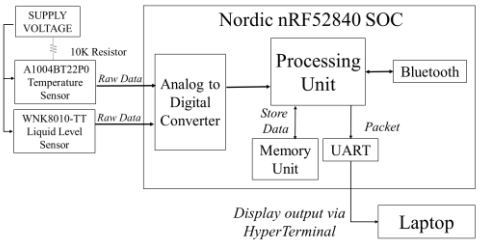

(a) Wireless IoT OLM System Block Diagram

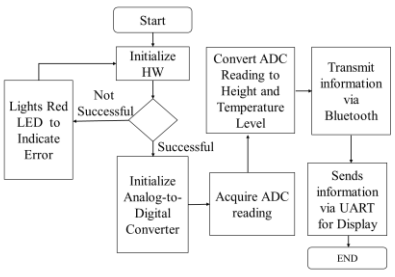

(b) Process Flowchart of OLM

Figure 3. OLM System Block Diagram & Process Flowchart

Firmware Process Flowchart

The Firmware implementation process flow chart of the OLM is illustrated in Fig. 3b. The implementation process begins with a series of initializations to the hardware device. This is to ensure that the device is functional. Once the microcontroller is running properly, the ADC settings are initialized, ready to measure the voltage information from the sensors. The translation of the voltage to temperature and liquid level are processed by two separate ADC ports. The conversion result is then sent via Bluetooth and displayed to a laptop HyperTerminal.

Though a more efficient wireless protocol like Wirepas may be used, the short-range wireless Bluetooth Technology Low Energy (BTLE) is employed in this study, making a more cost-effective battery-operated proof of concept. In the final application, the OLM may be an IoT node of a Smartgrid system which passes the sensor information collected wirelessly to an IoT gateway for data mining and further analysis in the cloud. Multiple OLMs may be used to form a mesh wireless network, to gather liquid level data from different equipment. In addition, I2C based sensors such as vibration, temperature, accelerometer, and the likes may be added to the OLM to monitor the other parameters of the pumps and generators along with the oil level.

III. Results and Discussion

Both the temperature and the hydrostatic sensors were characterized individually and then integrated into the Nordic SOC. The results are as follows:

A. Optimizing the System-On-Chip ADC Setting

How the Analog-Digital Converter (ADC) parameters are set affects the overall system performance of the SOC microcontroller, not just sensor accuracy. So, trade-offs between the other system functions such as wireless communication, memory management, hardware resource utilization etc. versus the ADC accuracy need to be optimized. In this study, the following ADC parameters were controlled: *oversampling*, *acquisition time*, *reference voltage*, and *gain*.

During the temperature sensor characterization, the ADC reading accuracy were compared with a calibrated Digital Multimeter (DMM) reading measuring the sensor output. The DMM reading represents the expected voltage values while the ADC readings are the measured values. Table 2 shows the difference of the expected and measured values at 25°C constant temperature.

TABLE II. NTC Reading Results: Measured Results vs. The Expected Value

Expected Voltage Reading (V)	Measured Voltage Reading (V)	Voltage Reading Difference (%)	Expected Temp. Reading (°C)	Measured Temp. Reading (°C)	Temp. Reading Difference (%)
1.6476	1.1997	27.1846	25.1000	38.2648	52.4494
1.6474	1.1997	27.1757	25.2000	38.2648	51.8444
1.6476	1.1997	27.1846	25.1000	38.2648	52.4494

The results show greater than 27% difference between the thermistor expected and measured voltage readings. This translates to a temperature inaccuracy reading by more than 50% which is outside the specified tolerance of ±5%. The ADC settings are as follows: an oversampling of 32 bit, an acquisition time of 3 uS, reference voltage of 0.6V, and gain of 0.5. These require adjustments. After several tests, the most optimal settings are the oversampling parameter is 64-bit, the acquisition time at 5 uS, the reference voltage at 0.6V, and the gain at 0.16. The result is shown in Table 3.

TABLE III. NTC Reading Results: Adjusted ADC Setting vs. The Expected Value

Expected Voltage Reading (V)	Measured Voltage Reading (V)	Voltage Reading Difference (%)	Expected Temp. Reading (°C)	Measured Temp. Reading (°C)	Temp. Reading Diff (%)
1.6467	1.6471	0.3427	25.1000	25.0810	0.6564
1.6460	1.6462	0.332	25.1000	25.1053	0.5597
1.6461	1.6453	0.3259	25.1000	25.1296	0.5597

These settings produced a very high level of accuracy, showing a temperature difference below 1%, which is within the ±5% tolerance requirement. The height ADC port setting used the same values considering the trade-offs of the overall system performance.

The ADC reading error includes the sensor error in a combined tolerance stack. Therefore, the error contribution of the sensor needs to be ascertained separately from the error contributed by the ADC to tightly control the tolerance stack.

B. Temperature Sensor Characterization

The temperature sensor used in this study is a 10K NTC thermistor - A1004BT22P0, from TE connectivity. Using a voltage divider circuit, a voltage reading is measured by the ADC input as the thermistor varies its resistance when the temperature changes.

The voltage measured, Vout, corresponds to the equation shown as:

$$\text{Vout} = \text{Vcc}\frac{R_{TH}}{(R+R_{TH})} \quad (1)$$

Where Vout is the output voltage measured by the ADC input port, R is the constant 10K 1% resistor, V_{CC} is the supply voltage, and R_{TH} is the thermistor resistance at a certain temperature. Table 4 shows the samples of the calculated Vout for the corresponding resistance and temperature of the NTC from the datasheet:

TABLE IV. NTC Resistance vs. Calculated Voltage

Temperature (°C)	Resistance (Ω)	Calculated Voltage (Vout)
125	340.6	0.10869582
100	678.4	0.20964939
50	3601	0.87370782
0	32650	2.52626026
-40	336050	3.20463806

However, one of the main challenges with using a thermistor is dealing with the thermal reading inaccuracy when calculating the temperature from the measured resistance value. Due to the nonlinear resistance-temperature (R-T) characteristics of the thermistor, inaccuracies are introduced at different points of the curve within the range.

To obtain a closer approximation of the thermistor temperature gauging, NTC uses the Steinhart-Hart equation during the conversion. It is regarded as the most precise empirical method for modeling the R-T characteristics of thermistors to a high degree of accuracy across the operational temperature range of the sensor. The equation is expressed in T where T is in degree Kelvin.

Steinhart - Hart Equation:

$$\frac{1}{T}=A+B(\ln R)+C(\ln R)^3 \quad (2)$$

Where T is the temperature in degree Kelvin, LnR is the natural logarithm of the measured resistance, and A, B, C are constants. The A, B, C constants are calculated based on the Temperature vs Resistance curve of the NTC datasheet.

$$\frac{1}{T_1}=A+B(\ln R_1)+C(\ln R_1)^3 \quad (3)$$

$$\frac{1}{T_2}=A+B(\ln R_2)+C(\ln R_2)^3 \quad (4)$$

$$\frac{1}{T_3}=A+B(\ln R_3)+C(\ln R_3)^3 \quad (5)$$

With,

T_1 = -40°C; at resistance (R_1) 336050 Ω of 10kΩ NTC
T_2 = 25 °C; at resistance (R_1) 10000 Ω of 10kΩ NTC
T_3 = 125°C; at resistance (R_1) 340.6 Ω of 10kΩ NTC

Solving for T using these three equations and three unknowns, we get the value of the constants:

A = 0.001129107098100
B = 0.000234126597883
C = 0.000000087702836

The Steinhart-hart equation with the constants above is encoded in the software to be used in the voltage-to-temperature conversion. The significance of this equation, along with the optimized ADC settings, is seen during the statistical analysis.

C. Liquid Level Hydrostatic Sensor Characterization

WNK8010-TT 1.5-S2-C2-05-D5 is the sensor used to measure the liquid level. The device voltage output characteristic range is 0.33V (the lowest level at 0 m) to 2.97V (the highest level at 1.5m / 60 inches). The sensor tolerance specification is 0.5% Full Scale (FS). This means that the reading accuracy is within ±0.5% of the full-scale reading. At 60-inch, the ±0.5% FS allowable error is ±0.30 inch across the range.

The liquid level is determined by the formula provided by the hydrostatic sensor manufacturer, as shown below:

$$LL=\frac{\frac{(V_R-V_{MIN})}{(V_{MAX}-V_{MIN})}*(H_{MAX}-H_{MIN})}{SG} \quad (6)$$

Where LL is the Liquid Level, V_R is the Voltage reading, V_{min} is the minimum voltage output of the sensor, V_{max} is the maximum voltage output of the sensor, H_{max} is the maximum sensor height capability, H_{min} is the sensor's minimum height capability, and SG is the specific gravity (SG) constant of the liquid medium. SG value changes depending on what liquid medium is used. SG for water is 1 while the SG varies for oil depending on the type and Manufacturer's hydraulic oil blend. SG is also a factor to control a much tighter reading accuracy. AW-32 Hydraulic Fluid (ISO 32) from O Reilly is used in this study. The full range (0-60 inch) height level is characterized using the Test Set-up 1. Some of the test readings are shown in Table 5.

TABLE V. HYDRO SENSOR READING RESULTS VS. THE EXPECTED READING

Expected Height Level (in.)	Expected Height Min. Level (in.)	Expected Height Max. Level (in.)	Hydro Sensor Reading (in.)	Results
0.1074	-0.19	0.41	0.27	In Range
12.7461	12.45	13.05	12.97	In Range
45.3405	45.04	45.64	45.64	In Range

The sensor performs within the manufacturer's tolerance specification. Due to safety concerns of handling hydraulic fluid at a large volume, water is used in taking the above measurements. However, a hydraulic fluid is used during the thermal characterization in Test set-up 2 (low volume).

D. Hydrostatic Sensor Issues due to Temperature Variations

The thermal characteristic of the hydrostatic sensor is assessed to determine the reading consistency and accuracy at varying thermal conditions. Three height levels were selected using Test Set-up 2. These are: Height A at 6 inches, Height B at 4 inches, and Height C at 2 inches, taken across the temperature requirement from -15 to 70 °C. Table 6 shows three of the Height A data points taken from the whole temperature range:

TABLE VI. HEIGHT A SENSOR READINGS AT DIFFERENT TEMPERATURE LEVELS

Height A (in.)	Temperature Level (°C)	Voltage Reading (V)	Height Reading (in.)	Error from Height A (%)
6	70	0.4734	4.2934	28.44%
6	25	0.5325	6.0383	0.64%
6	-15	0.4348	3.1266	47.89%

Notice that at temperatures 70°C and -15°C more than 8 % error occurred from the desired height. This does not meet the specification. Similar behavior occurred during the characterization of Heights B and C with even higher inaccuracies. These show that the thermal variations affect the sensor performance.

E. Applying the Correction Factor, CF

By reviewing the graphs, a trend is observed. Fig. 4 below shows the trend of the three height levels vs Temperature.

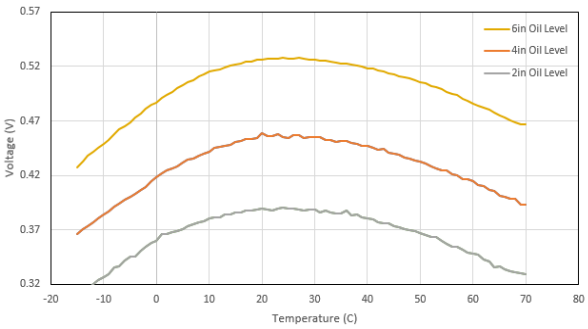

Figure 4. Point A, B, and C, result curves at -15°C to 70 °C.

By aligning Heights B and C graphs to Height A, a common curve is derived. From this curve, a trendline is determined to formulate the correction factor, CF. Taking the average of the data points on the curve, the corresponding characteristic equation is derived:

$$\gamma=3.65E\text{-}12x^6-6.98E\text{-}10x^5+4.76E\text{-}8x^4-9.9387E\text{-}7x^3-6.1284E\text{-}5x^2+3.08E\text{-}3x+0.4912 \quad (7)$$

Where x is the temperature level read and y is the height level calculated at that temperature. This is illustrated in Figure 5a.

Since the horizontal tangent line is the highest point of the curve (i.e., the closest value to the expected height level), by taking the first derivative, the equation of the tangent line is derived:

$$\gamma'=2.1877E\text{-}11x^5-3.492E\text{-}9x^4+1.9054E\text{-}7x^3-2.982E\text{-}6x^2-1.226E\text{-}3x+0.00308 \quad (8)$$

Where x is the temperature level read and y' is the normal height level to the curve, i.e., the highest point of the curve at that temperature. This point is the closest approximation to the expected height level.

The steps then to determine the final corrected levels are:

a) Use the trend line equation to determine the liquid level (y) at a given temperature (x). This is the initial height reading.
b) Use the normal horizontal line equation to determine the highest point of the curve (y') from (x).
c) Take the difference of the trend line result (y) and the normal horizontal line (y'). This is the correction factor.
d) Add the correction factor to the initial reading (y) from step (a). This is now the final corrected level.

Fig. 5b shows the measured and new adjusted heights for Height A, 6-in.

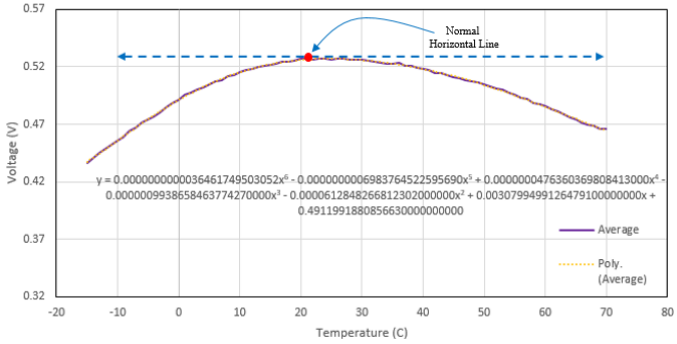

(a) Average Curve of All Three Levels with the Trendline Equation and Horizontal Tangent Line

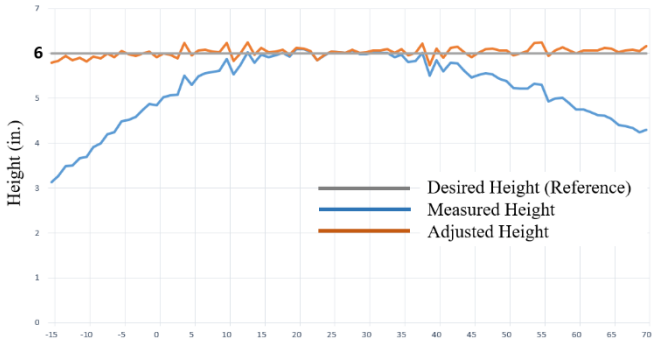

Height A Test Result with and without CF.

(b) Measured (no CF) and adjusted height (with CF) vs. the target H_A = 6" (Horizontal Tangent Line) Test Result.

Figure 5 Average Curves and Trendline from the Three height levels

Tables 7, 8, & 9 summarize the improvements when applying the CF to the measured data and optimizing SG:

TABLE VII. H_A = 6" SENSOR READING IMPROVEMENT (NO CF VS WITH CF)

Temperature (°C)	Error from 6-in. (no CF) % (Reading, in.)	Error from 6-in. (with CF) % (Reading, in.)
70	28.44% (4.29 in.)	2.62% (5.84 in.)
25	0.64% (5.96 in.)	0.64% (5.96 in.)
-15	47.89% (3.13 in.)	3.40% (5.80 in.)

TABLE VIII. H_B = 4" SENSOR READING IMPROVEMENT (NO CF VS WITH CF)

Temperature (°C)	Error from 4-in. (no CF) % (Reading, in.)	Error from 4-in. (with CF) % (Reading, in.)
70	47.78% (2.09 in.)	1.18% (3.95 in.)
25	0.76% (Reads at 3.97 in.)	0.77% (3.97 in.)
-15	66.68% (Reads at 1.33 in.)	0.06% (3.99 in.)

TABLE IX. H_C = 2" SENSOR READING IMPROVEMENT (NO CF VS WITH CF)

Temperature (°C)	Error from 2-in. (no CF) % (Reading, in.)	Error from 2-in. (with CF) % (Reading, in.)
70	28.44% (1.43 in.)	4.27% (1.91 in.)
25	0.64% (1.99 in.)	5.36% (1.89 in.)
-15	47.89% (1.04 in.)	11.26% (1.77 in.)

The inaccuracy is now reduced to well within the 8% requirement except, the -15°C reading at the 2-in. level still shows an error greater than 8%, even though the readings generally improved. The reasons for this behavior are: 1) At 0 or near minimum level, the noise margin of the sensor is also nearing its noise floor. It is noticed that the sensor accuracy degrades from about the 3-in. level down. 2) At low temperature, the oil viscosity increases, changing from liquid to gel below around -8 °C and behaves as a thicker fluid.

F. Statistical Treatment

Performance Capability (C_p) and Capability Index (C_{pk})

The DFSS Performance Capability (Cp) and Capability Index (Cpk) are objective statistical measurements to determine if the design is meeting the requirement. The Performance Capability is the ratio of the required versus the actual performance of the sensor. The Performance Capability Index (Cpk) is a measure of the ability of the sensors to produce consistent results between the permissible specified spread (i.e., the total tolerance specification) and the actual spread (Performance Limit). A Cpk has Upper (Cpk USL) and Lower Limits (Cpk LSL) for off-target variations. These limits are calculated values to signify if the variations of the collected data are centered between the specified limits. It is used to estimate how close the sensor performance is to a given target and how consistent the sensor measurement is around the average performance. Cp provides the overall idea of how capable the sensor performances are in meeting the requirement while Cpk defines how centered the measured readings are within the specified range. The controlling factors may be adjusted to come up with the value of Cp > 1, which demonstrates a more than capable performance within the specification. A Cp = 1 means the performance is capable with no margin and requires tight control. A Cp < 1 indicates that the performance capability spread is greater than the specification which means poor capability. A Cpk of negative value means that the performance capability is outside the specified limits, drifting either at the upper or lower end. A Cpk of 1 means that the device is just touching the nearest edge of the limits not having enough clearance and may likely fail. A Cpk of 2 (6 σ) means that there is a large amount of clearance. Whichever limit is of the lower value means that the design control shifted in that direction and highly likely the performance will fail at that limit. Therefore, the lower of the two values is noted, design adjustments are made making trade-offs accordingly to shift the performance toward the center of the limits. A Cpk value greater than 1.33 (4 σ) is desirable in this study. Fig. 6 below summarizes the C_p and C_{pk} concept and relationships.

$$Cp = \frac{SPECIFICATION\ LIMIT}{PERFORMANCE\ LIMIT} = \frac{(upper\ spec - lower\ spec)}{n\,\sigma}$$

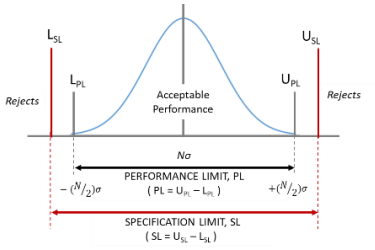

Good Performance Capability

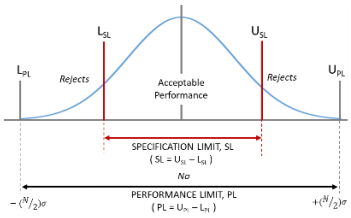

Poor Performance Capability

$$Cpk = min\left[\frac{(upper\ spec - mean)}{\frac{n}{2}\sigma}, \frac{(mean - lower\ spec)}{\frac{n}{2}\sigma}\right]$$

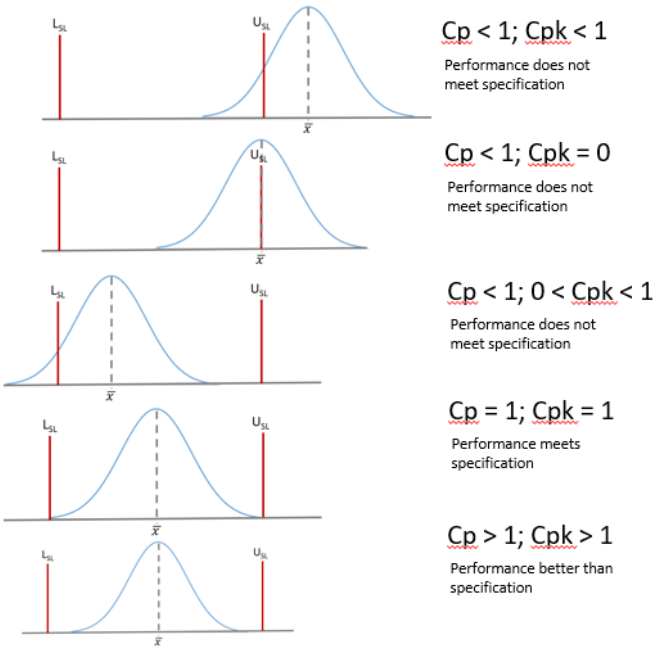

Figure 6. Cp and Cpk Correlations

In this study, the specification for the height and temperature readings are ±8% and ±5%, respectively. By using the C_p / C_{pk} analysis, the adjustments applied to the controlling parameters made the performance meet the specification and improved them even further.

1. Temperature Monitor Performance Capability

Prior to optimizing the ADC and adding the Steinhart-Hart (S-H) equation, the temperature readings were taken across the required range. The statistical analysis shows C_p and C_{pk} equal to 0.28 resulting to a distribution curve that is well out of the specification. The measured data drifts more than 50% of the expected value to the right of the Upper Specification Limit (U_{SL}), as illustrated in Fig. 7a.

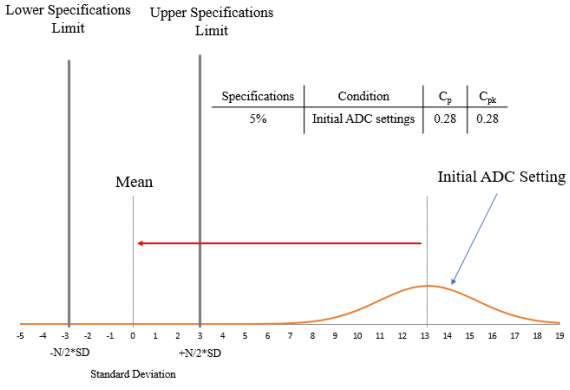

(a) Distribution Curve: Pre-optimized ADC setting, without S-H equation

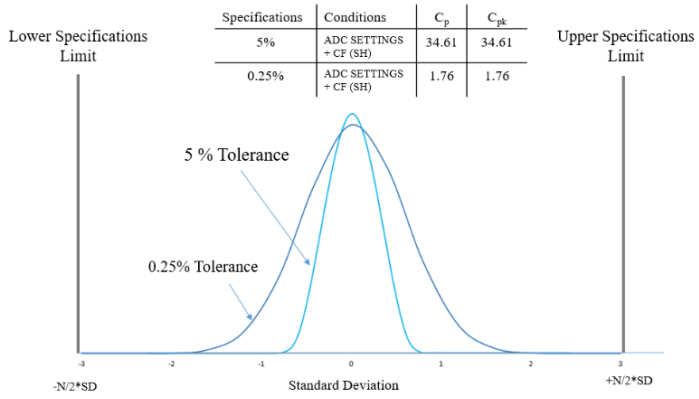

(b) Distribution Curve: Post-optimized ADC Setting, with S-H equation

Figure 7. Distribution Curves for ADC Settings, with & without S-H equation

After applying the Steinhart-hart equation and adjusting the ADC settings, the Cp and Cpk greatly improved within the specification of ±5%. Since there is enough room for improvement, the data was re-evaluated using a tighter specification limit. The optimized result shows that the temperature sensor can perform well within ±0.25% tolerance limits as shown in Figure 7b.

2. Liquid Level Monitor Performance Capability

The Performance Capability analyses were also performed when determining the CF at Heights A (6”), B (4”), and C (2”). Considering Height A experiment for example, 86 data points from -15 to 70 °C were taken. With no CF, the Cp and Cpk are equal to 0.37, in which case the distribution curve is out of specification, is not centered and drifting more to the right side of the limits, as illustrated in Fig. Figure 8a.

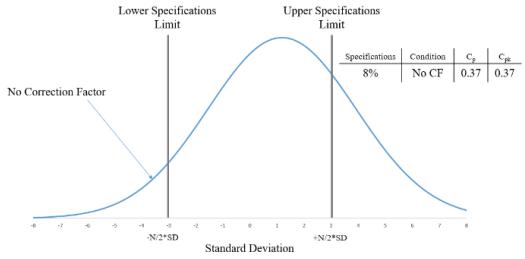

(a) Distribution Curve results of Height A without the correction factor at 8% specification limits

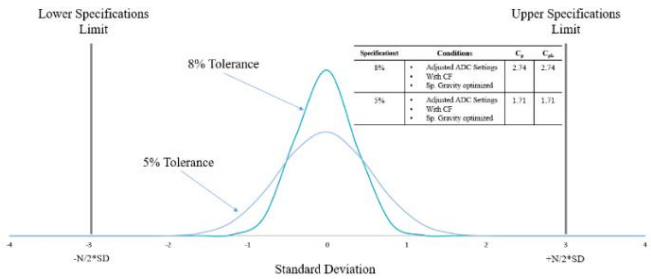

(b) Distribution Curve results of Height A with the correction factor compared with 8% and 5% specification limits

Figure 8. Distribution Curve Results of Height A (6 inches)

After adjustments were made to SG, the ADC settings, and adding the equation for the CF in the code, the performance capability improved with Cp and Cpk equal to 2.74 best case, with SG as the fine-tuning parameter. This improvement translates to a mean from 5.2115 inches to 6.0281 inches, a

much closer value to 6 inches. With this configuration, the system performance is very capable of meeting the ±8% design specification. Moreover, a much tighter specification of ±5% is possible, resulting in Cp and Cpk equal to 1.71, as illustrated in Fig. 8b.

G. Full Scale 1.5m (60 IN) Hydrostatic Sensor Test

Finally, after all the optimization and correction factors are applied in the code, a full-scale reading verification test was conducted across the range from 0 to 60 inches with water. The sample data of the test results in Table 10 show the OLM height readings meet the ±8% specification limits and the ±0.5% FS tolerance (±0.30 inch) of the hydrostatic sensor.

TABLE X. FULL-SCALE MEASUREMENT AT ROOM TEMPERATURE SAMPLE DATA

Height Level (in.)	Required Min. -8% (in.)	Required Max. +8% (in.)	Sensor Min. Spec. (in.)	Sensor Max. Spec. (in.)	OLM Height Reading (in.)	Result
4.00	3.68	4.32	3.70	4.30	4.01	In range
25.00	23.00	27.00	24.70	25.30	25.03	In range
60.00	55.20	64.80	59.70	60.30	60.19	In range

DFSS Performance Capability processes and analyses effectively aid in determining the optimal settings for the ADC parameters, the specific gravity (SG) values, and the derivation of the correction factors for the height and temperature equations.

IV. RECOMMENDATION AND CONCLUSION

In this study, there are factors in the design that affect the accuracy of the readings. They are controlled to achieve the optimal solution. These factors are: 1) the microcontroller ADC settings, 2) the non-linearity effects of the thermal variations to the hydrostatic level sensor, 3) the non-linearity effects of the R-T characteristics of the thermistor, and 4) regulating the specific gravity (SG) value to achieve a more precise liquid level reading. With the use of the DFSS Cp / Cpk statistical analysis, the sensor readings were highly improved by calibrating the microcontroller configurations considering the trade-offs between ADC conversion accuracy versus the overall hardware resource performance. A correction factor CF is added in the hydrostatic sensor conversion code to compensate for the thermal drifts, reducing the errors across the temperature range meeting and even performing better than the 8% specification. Similarly, a more precise empirical model, the Steinhart-hart equation, was added in the voltage-to-temperature conversion code of the temperature sensor, which improved the error to less than 1%. The efficacy of these adjustments was evident as the sensors' Cp / Cpk values highly improved. However, at the 2-in. level and below, the hydrostatic sensor performance is limited due to the noise margin constraints near or at minimum level and the change of oil viscosity at low temperature. It is recommended to further characterize the sensor at low level and low temperature applications. Machine learning was considered to improve the accuracy of the sensor readings, but the processing power required to manage the computing and communication tasks is too high for a battery-operated device. Further study on managing non-linear behavior of sensors in a low energy battery operated environment using machine learning is a logical next step and highly recommended.

Moreover, water is used instead of oil as the medium for the full-scale (0-60 inch) verification testing. Proper material handling for health and safety is required when working with hazardous material in large volumes. In addition, due to the size of the container at large volume, full-scale test is done at room temperature only (25~27 °C) as a large thermal chamber that fits the container is not available. No temperature tests from -15 to 70 °C were conducted in this study at levels greater than 6 inches due to the size limitation of the available thermal chamber. It is recommended to test the maximum height against temperature when a suitable setup is available.

By not using inline piping sensors so as to make no changes to the tank or pipe structural integrity, the study concludes that a wireless mixed-signal SOC with submersible hydrostatic and NTC temperature sensors enclosed in a housing mounted on top of the tank is a viable solution for a non-invasive IoT oil level monitor. In addition, what this study reveals, is that the DFSS Performance Capability (Cp) and Capability Index (Cpk) statistical analysis from the outset is an effective method to determine the appropriate settings in compensating for the non-linearity effects of the sensors and obtain the most optimal reading performance.

V. REFERENCES

[1] Roland Berger, "Mastering the Industrial Internet of Things (IIoT)" Sederanger, 80538 Munich, Germany, 2017.

[2] Yang Li, Meng Gao, Licheng Yang, Cuiping Zhang, Bo Zhang, Xiaonan Zhao, "Design of and research on industrial measuring devices based on Internet of Things technology.", College of Electronic and Communication Engineering, Tianjin Normal University, Tianjin 300387, China, 2020.

[3] Komal S. Shinde, Prachi H. Bhagat, "Industrial Process Monitoring Using IoT.", Department of Electronics & Telecommunication Government College of Engineering, Aurangabad, Maharashtra, India, 2017.

[4] Carlo N. Cabaccan, Febus Reidj G. Cruz, Ireneo C. Agulto, "Wireless Sensor Network for Agricultural Environment using Raspberry Pi based Sensor Nodes.", School of Electrical Electronics and Computer Engineering, Mapua University, Intramuros, Manila, Philippines, 2017.

[5] Jennifer C. Dela Cruz, Glenn V. Magwili, Kyle C. Catimbang, Terrence Bosser S. Serrano, Paul Christian L. Reyes, "Solar Lamp Post Health Monitoring Using Integrated Sensors and Wireless Network.", 2021 IEEE 17th International Colloquium on Signal Processing & Its Applications (CSPA), 5 - 6 March 2021

[6] Cheryl Tayo, Novie Dave Perez, Jocelyn Villaverde, "Design and Development of a WSN for Water Quality Monitoring System of Shrimp Aquaculture", School of EECE Mapúa University, Manila, Philippines. Proc. of the International Conference on Electrical, Computer and Energy Technologies (ICECET 2022) 20-22 July 2022, Prague-Czech Republic

[7] Karl Justine S. Agapito, Gabriel V. Balao-a, Eugene Jason A. Enriquez, Paulo Rafael Meris, Mark Christian E. Manuel' Rodrigo S. Pangantihon Jr., Jocelyn F. Villaverde, " Development of a Wireless Magnetic Climbing Robot for Visual Inspection of Galvanized Cooling Towers in a Commercial Building", School of Mechanical and Manufacturing Engineering, School of Graduate Studies, School of Electrical, Electronics, and Computer Engineering, Mapúa University Manila, Philippines

[8] Chad Ferrino P. Abuda, Meo Vincent S. Caya, Febus Reidj G. Cruz, Francis Aldrine A. Uy, "Compression of Wireless Sensor Node Data for Transmission based on Minimalist, Adaptive, and Streaming Compression Algorithm", School of Electrical, Electronics, and Computer Engineering, Mapua University, Manila, Philippines, 2019.

[9] Zhao Jinxiang, Sun chuanwei, and Steve W. Y. Mung, "Research on Elevator General Uninterrupted Safety System Based on Zigbee andInternet", 2017 IEEE 2nd International Conference on Signal and Image Processing, 2017

[10] Samik Marick, Saikat Kumar Bera, Satish Chandra Bera, "A Float Type Liquid Level Measuring System Using a Modified Inductive Transducer", Sensors & Transducers, Vol. 182, Issue 11, November 2014, pp. 111-118.

[11] S. Faizan Ali, and N. Mandal, "Design and development of an electronic level transmitter based on hydrostatic principle," Indian Institute of Technology (ISM), Dhanbad, Department of Electronics Engineering, Dhanbad 826004, Jharkhand, India.

[12] Yadvendra Singh, Soubir Kumar, Sanjeev kumar Raghuwanshi, "Review on Liquid-level Measurement and Level Transmitter Using Conventional and Optical Techniques", Article in IETE Technical Review · June 2018.